Theoretical analysis of scanning capacitance microscopy

H. E. Ruda and A. Shik*
Electronic Material Group, University of Toronto, Toronto M5S 3E4, Canada
(Received 10 January 2003; published 10 June 2003)

A theoretical analysis of scanning capacitance microscopy is presented. By solving and matching the corresponding Laplace and Poisson equations for vacuum and semiconductor, the potential and charge distributions induced by a rounded tip in a semiconductor sample were found and used to calculate the capacity and its voltage derivative. The results allow us to analyze the dependence of the capacitance on the semiconductor doping level, applied voltage, and tip geometry, and to estimate the spatial resolution of such measurements.

DOI: 10.1103/PhysRevB.67.235309 PACS number(s): 73.63.Rt, 41.20.Cv, 84.37.+q

I. INTRODUCTION

Scanning capacitance microscopy (SCM) is a modern characterization technique commonly used for analyzing doping profiles in semiconductor-based structures.[1] Its wider application is, however, limited by the absence of a comprehensive theory describing the local capacity measured by SCM, its dependence on sample parameters, measuring tip characteristics, and its spatial resolution. The theoretical basis of SCM has been restricted to some numerical calculations[1–5] without strictly formulated starting assumptions, which does not allow one to estimate their feasibility and trace the underlying behavior for this method. The only paper containing analytical results[6] describes the electric field distribution outside of a sample but does not treat screening in it and hence cannot be applied to the problems of semiconductor diagnosis. In this work we develop an analytical theory of SCM describing the measured capacity and its derivatives, their dependence on the applied voltage, sample doping, and tip characteristics, as well as establishing the spatial resolution of the method.

II. POTENTIAL DISTRIBUTION IN VACUUM

A. General solution

The theoretical analysis of SCM begins with a determination of the potential distribution between the tip and sample, and charge distribution in them. For this purpose a simple model, which considers the tip as a metallic sphere, is usually applied (see, e.g., Ref. 1). However, this model describes a tip by a single parameter—curvature radius R which is also the external dimension of the electrode. This is an inadequate description since, as will be shown below, the measured capacity is determined by the macroscopic dimensions of the electrode, which in real structures may exceed the tip curvature radius by orders of magnitude. Moreover, even for this simple spherical model, the authors do not discuss an analytical solution, which could be found for this simple geometry and would provide the dependences on R and on the distance d between the electrode and the sample, but restrict themselves to some numerical results.

We solve analytically a more realistic model where the tip curvature is not related to the electrode size and can be varied independently. In this model the electrode surface is considered as a hyperboloid of one sheet of revolution (Fig. 1). We use the prolate spheroidal system of coordinates (ξ,η,ϕ) where ϕ is the angle or rotation about the z axis while $1 \leqslant \xi < \infty$ and $-1 \leqslant \eta \leqslant 1$ are related to the cylindrical coordinates (ρ,z) by the transformation

$$\rho = \frac{a}{2}\sqrt{(1-\eta^2)(\xi^2-1)}, \quad z = \frac{a}{2}\xi\eta. \tag{1}$$

For a given R and d, the parameter $a = 2\sqrt{d^2+Rd}$, and the sample and tip surfaces correspond to $\eta = 0$ and $\eta = (1+R/d)^{-1/2}$, respectively. If we assume that metallic tip has the potential V relative to the sample, to find the spatial distribution of the potential $\varphi_+(\xi,\eta)$ (the subscript $+$ indicates the semispace $z>0$), we solve the Laplace equation $\Delta\varphi_+ = 0$ with the boundary condition

$$\varphi_+[\xi,(1+R/d)^{-1/2}] = V. \tag{2}$$

Other conditions require finiteness of φ_+ at $\xi = 1$ (the axis $\rho = 0$) and at $\xi \to \infty$ and matching with the potential distribution in semiconductor ($z<0$).

For these boundary conditions the variables in the Laplace equation can be separated: $\varphi_+(\xi,\eta) \sim R(\xi)S(\eta)$, where both $R(\xi)$ and $S(\eta)$ are to be found from the same ordinary differential equation[7]

$$(1-x^2)y'' - 2xy' + \nu(\nu+1)y = 0.$$

Its solution is given in terms of Legendre functions of the first $P_\nu(x)$ and the second $Q_\nu(x)$ kind. In our case ξ can acquire any value equal to or exceeding 1. For this reason $R(\xi) \sim P_\nu(\xi)$ and contains no Q_ν since all $Q_\nu(\xi)$ are singular at $\xi = 1$. For $R(\xi)$ to remain finite at $\xi \to \infty$, the parameter ν must lie between -1 and 0. Since $P_\nu(\xi) = P_{-\nu-1}(\xi)$ (see, e.g., Ref. 8), all nonequivalent eigenfunctions of our problem fall within the interval

$$-1/2 \leqslant \nu \leqslant 0.$$

The argument of $S(\eta)$ varies from 0 to $(1+R/d)^{-1/2} < 1$. For this reason, $S(\eta)$ may contain both $P_\nu(\eta)$ and $Q_\nu(\eta)$. After applying the boundary condition (2), the following expression for the potential is obtained:

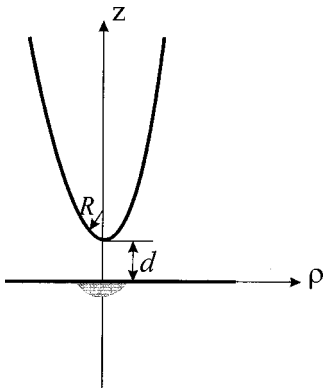

FIG. 1. Schematic illustration of SCM measurements. The shaded area corresponds to the space charge region in the semiconductor sample.

$$\varphi_+(\xi,\eta)=\int_{-1/2}^{0}A(\nu)P_\nu(\xi)\left[P_\nu(\eta)-\frac{P_\nu[(1+R/d)^{-1/2}]}{Q_\nu[(1+R/d)^{-1/2}]}Q_\nu(\eta)\right]d\nu+V, \quad (3)$$

where $A(\nu)$ is determined by the boundary condition at the interface $z=0$ $(\eta=0)$. For capacity calculations the total potential distribution is not needed, but only the electric field at the sample interface:

$$\begin{aligned}F(\xi)&=-\frac{\partial\varphi_+}{\partial z}(z=0)\\&=-\frac{1}{\xi\sqrt{d^2+Rd}}\frac{\partial\varphi_+}{\partial\eta}(\eta=0)\\&=-\frac{\sqrt{\pi}}{\xi\sqrt{d^2+Rd}}\int_{-1/2}^{0}A(\nu)P_\nu(\xi)\frac{\Gamma\left(1+\frac{\nu}{2}\right)}{\Gamma\left(\frac{1}{2}+\frac{\nu}{2}\right)}\\&\quad\times\left[\frac{2}{\pi}\sin\left(\frac{\pi\nu}{2}\right)-\frac{P_\nu[(1+R/d)^{-1/2}]}{Q_\nu[(1+R/d)^{-1/2}]}\cos\left(\frac{\pi\nu}{2}\right)\right]d\nu\end{aligned} \quad (4)$$

determining the induced charge.

B. A "metallic" sample

Equation (3) can be used to calculate the tip self-capacity C_0, i.e., the capacity between the tip and a planar metallic electrode having a very small screening length which has no influence on the measured capacity, which in this case is caused exclusively by geometric characteristics of the instrument. The metallic electrode is an equipotential surface, so that $\varphi_+(\xi,0)=0$. For this case in Eq. (3), $A(\nu)=-V\delta(\nu)$ and

$$\varphi_+^0(\eta)=V\frac{\ln\left(\frac{1+\eta}{1-\eta}\right)}{\ln\left(\frac{\sqrt{d+R}+\sqrt{d}}{\sqrt{d+R}-\sqrt{d}}\right)}=\text{const}(\xi). \quad (5)$$

For this potential distribution the profile of charge density at the $z=0$ plane can easily be found:

$$\begin{aligned}\sigma_0(\rho)&=-\frac{1}{4\pi}\left(\frac{\partial\phi_0}{\partial z}\right)_{z=0}\\&=-\frac{V}{2\pi\ln\left(\frac{\sqrt{d+R}+\sqrt{d}}{\sqrt{d+R}-\sqrt{d}}\right)\xi\sqrt{d^2+Rd}}\\&=-\frac{V}{2\pi\ln\left(\frac{\sqrt{d+R}+\sqrt{d}}{\sqrt{d+R}-\sqrt{d}}\right)\sqrt{\rho^2+d^2+Rd}}.\end{aligned} \quad (6)$$

By integrating Eq. (6) over the whole interface the total induced charge can be found and, hence, the electrode capacity C_0. For infinite integration limits the solution is divergent, but if we restrict the integration to some radius r_m, as determined by the size of electrode, then

$$C_0=\frac{2\pi}{V}\int_0^{r_m}|\sigma_0(\rho)|\rho d\rho=\frac{(\sqrt{r_m^2+d^2+Rd}-\sqrt{d^2+Rd})}{\ln\left(\frac{\sqrt{d+R}+\sqrt{d}}{\sqrt{d+R}-\sqrt{d}}\right)}. \quad (7)$$

In the limit of a very large curvature radius $R\gg r_m$, d, Eq. (7) reduces to the formula for a plane capacitor $C_0=r_m^2/(4d)$.

In the following sections we discuss changes in the tip capacity caused by the screening effects in a nonmetallic (semiconductor) sample and information on the sample parameters that can be extracted from the capacity measurements. However, already some general remarks can be made. We see that the main contribution to C_0 originates from distant regions with large ρ. For these regions the distance to the tip exceeds the screening length in the semiconductor so that the influence of screening is negligible and local values of the surface charge density are given by Eq. (6). This means that the values of tip capacity are, in fact, determined by the macroscopic geometry of instrument, providing for very poor spatial resolution even for a very thin tip and containing no information on the doping level and other characteristics of the sample. It will become apparent that in order to avoid these difficulties and measure the semiconductor characteristics with sufficient resolution, modulation methods need be used.

C. Smooth potential

In Sec. II B we discussed the limiting case of an equipotential semiconductor surface when $A(\nu)=-V\delta(\nu)$. Now we consider the situation when the potential at the interface $\varphi_+(\xi,0)$ is not constant but varies slowly, at characteristic

distances considerably exceeding R and d. This is a rather realistic assumption. Many commercial SCM instruments are multiprobe instruments used simultaneously for scanning tunnel microscopy (STM) and atomic force microscopy (AFM), where R and d lie in nanometer region. At the same time, the characteristic distance of potential variations within the semiconductor is the screening length λ^{-1} (see Sec. III), which in moderately doped semiconductors is at least an order of magnitude larger. This means that we are really interested in values $\xi \gg 1$. Using the corresponding asymptotic formula for $P_\nu(\xi)$, gives

$$\varphi_+(\xi,0)=\frac{1}{\pi}\int_{-1/2}^{0}(2\xi)^{\nu}A(\nu)\frac{\Gamma\left(\frac{1}{2}+\frac{\nu}{2}\right)\Gamma\left(\frac{1}{2}+\nu\right)}{\Gamma\left(1+\frac{\nu}{2}\right)\Gamma(1+\nu)} \times\left[\cos\left(\frac{\pi\nu}{2}\right)-\frac{\pi P_\nu[(1+R/d)^{-1/2}]}{2Q_\nu[(1+R/d)^{-1/2}]}\times\sin\left(\frac{\pi\nu}{2}\right)\right]d\nu+V. \tag{8}$$

Similarly,

$$F(\xi)=-\frac{2}{\pi\xi\sqrt{d^2+Rd}}\int_{-1/2}^{0}(2\xi)^{\nu}A(\nu)\frac{\Gamma\left(1+\frac{\nu}{2}\right)\Gamma\left(\frac{1}{2}+\nu\right)}{\Gamma\left(\frac{1}{2}+\frac{\nu}{2}\right)\Gamma(1+\nu)} \times\left[\sin\left(\frac{\pi\nu}{2}\right)-\frac{\pi P_\nu[(1+R/d)^{-1/2}]}{2Q_\nu[(1+R/d)^{-1/2}]}\cos\left(\frac{\pi\nu}{2}\right)\right]d\nu. \tag{9}$$

At $\xi \gg 1$ the main contribution to the integrals of Eqs. (8) and (9) is given by small $|\nu|$ and to good approximation, one can replace all ν-dependent factors except $(2\xi)^{\nu}A(\nu)$ with their values at $\nu=0$, giving

$$F(\xi)=\frac{2[\varphi_+(\xi,0)-V]}{\ln\left(\frac{\sqrt{d+R}+\sqrt{d}}{\sqrt{d+R}-\sqrt{d}}\right)\xi\sqrt{d^2+Rd}} =\frac{2[\varphi_+(\xi,0)-V]}{\ln\left(\frac{\sqrt{d+R}+\sqrt{d}}{\sqrt{d+R}-\sqrt{d}}\right)\sqrt{\rho^2+d^2+Rd}}. \tag{10}$$

The expression (10) generalizes Eq. (6) to the case of a smoothly varying boundary potential, giving the linear connection between the potential and its normal derivative at the interface. This allows us, in all further analysis, to consider only the potential distribution within the sample (at $z<0$) using Eq. (10) as the boundary condition which contains all of the information on the potential in vacuum and on the tip parameters.

III. SCREENED POTENTIAL IN A SEMICONDUCTOR

A. Linear and quasilinear screening

The potential profile induced by the tip inside a semiconductor ($z<0$) is now considered. We assume that the material is n type with an electron concentration n_0 causing effective screening of the tip-induced electric field. For nondegenerate electrons the equation for this cylindrically symmetric potential $\varphi_-(\rho,z)$ is

$$\frac{1}{\rho}\frac{\partial}{\partial\rho}\left(\rho\frac{\partial\varphi_-}{\partial\rho}\right)+\frac{\partial^2\varphi_-}{\partial z^2}=\frac{kT\lambda^2}{e}\left[\exp\left(\frac{e\varphi_-}{kT}\right)-1\right], \tag{11}$$

where $\lambda=(4\pi n_0 e^2/\varepsilon kT)^{1/2}$ is the inverse screening length and ε is the semiconductor dielectric permittivity. The solution for this potential should match that for the potential distribution in vacuum, as found in Sec. II. Since the latter satisfies the boundary condition (10), it results in the following boundary condition for φ_-:

$$\left(\frac{\partial\varphi_-}{\partial z}\right)_{z=0}=-\frac{2[\varphi_-(\rho,0)-V]}{\varepsilon\ln\left(\frac{\sqrt{d+R}+\sqrt{d}}{\sqrt{d+R}-\sqrt{d}}\right)\sqrt{\rho^2+d^2+Rd}},$$

$$\varphi_-(z\to-\infty)=0. \tag{12}$$

The problem is easily solved for small applied voltage V (of any sign) when the right side of Eq. (11) can be linearized. In this case (corresponding to the well-known Debye approximation), the general solution of Eq. (11) is

$$\varphi_-^{(1)}(\rho,z)=\int_0^\infty A(t)\exp(-\sqrt{t^2+\lambda^2}|z|)J_0(t\rho)dt, \tag{13}$$

where $A(t)$ can be found from the boundary condition of Eq. (12). The superscript (1) in Eq. (13) indicates the first-order, linear in V, character of our approximation. The problem has no general analytical solution but can be simplified noticeably in the case when the applied voltage V is dropped mostly at the dielectric interval between the tip and the sample, and only a minor part of it is screened within the sample. This approach is *a priori* adequate for a relatively large d but, as we will show later, its applicability is considerably wider including, in particular, the case of a very sharp tip. This means that the term $\varphi_-(\rho,0)$, on the right-hand side of Eq. (12), can be omitted and $A(t)\varphi_-(\rho,0)$ can be determined giving

$$\varphi_-^{(1)}(\rho,z)=\frac{2V}{\varepsilon\ln\left(\frac{\sqrt{d+R}+\sqrt{d}}{\sqrt{d+R}-\sqrt{d}}\right)} \times\int_0^\infty\frac{\exp(-t\sqrt{d^2+Rd}-\sqrt{t^2+\lambda^2}|z|)}{\sqrt{t^2+\lambda^2}}J_0(t\rho)dt. \tag{14}$$

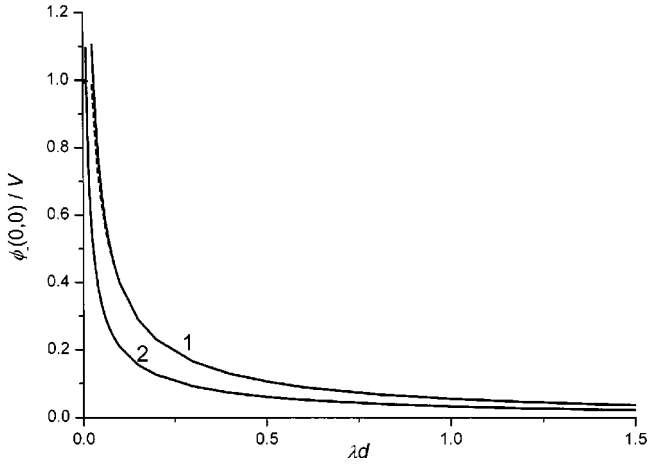

FIG. 2. Relative voltage drop in the semiconductor sample for two tip radii: $\lambda R=1$ (curve 1) and $\lambda R=0.1$ (curve 2). The dashed lines represent an interpolation for small d.

We use Eq. (14) for finding the applicability limits for this expression. To do this, we take the maximal value of $\varphi_-^{(1)}\times(\rho,z)$ realized at the origin (0,0) and require it to be much less than V. Figure 2 shows $\varphi_-^{(1)}(0,0)/V$ calculated for different relationships between d, R, and λ, when $\varepsilon=12$, as is typical for most semiconductors. This shows that the approximation is adequate not only for $d\lambda>1$, which is clear, but also for a tip with a very small radius of curvature R. For nanoscopes with R lying in nanometer region, the abovementioned limits may be sufficiently wide. At very small d, Eq. (14) becomes inadequate, and $\varphi_-^{(1)}(0,0)$ tends to V, as shown by the dashed lines in Fig. 2.

The case of linear screening will be used below to provide a number of important estimates, although it cannot be directly used for capacity calculations. As we have already mentioned in Sec. II, the total charge and hence the tip capacity as determined by Eq. (5), as well as by Eq. (14), has the same asymptotic behavior at large ρ, and is divergent. It cannot, therefore, be used for determination of the sample parameters. The latter can be found only from differential characteristics, e.g., dC/dV, which will be the main focus of further calculations. But in the linear case, C is independent of the applied voltage, and so this approach is inapplicable. Thus, all SCM measurements and their theoretical description should be conducted under nonlinear conditions, which will be discussed in the following subsection.

B. Adiabatic approximation

An analytical solution of Eq. (11) at large applied voltages can be obtained in the adiabatic approximation assuming that the potential varies in the z direction much faster than along the interface. In this case, we can neglect the ρ derivatives in Eq. (11) and integrate once the resulting ordinary differential equation. Its solution, for which both φ_- and $d\varphi_-/dz$ vanish simultaneously at $z\to-\infty$, connects these parameters at $z=0$:

$$\frac{e}{\sqrt{2}kT\lambda}\left(\frac{\partial\varphi_-}{\partial z}\right)_{z=0}=\mathrm{sgn}(V)\sqrt{\exp\left[\frac{e\varphi_-(\rho,0)}{kT}\right]-1-\frac{e\varphi_-(\rho,0)}{kT}}. \tag{15}$$

By excluding $d\varphi_-/dz$ from Eqs. (12) and (15) we obtain the equation for the surface potential $\varphi_-(\rho,0)$

$$\frac{\sqrt{2}e[V-\varphi_-(\rho,0)]}{\lambda\varepsilon kT\ln\left(\frac{\sqrt{d+R}+\sqrt{d}}{\sqrt{d+R}-\sqrt{d}}\right)\sqrt{\rho^2+d^2+Rd}}=\mathrm{sgn}(V)\sqrt{\exp\left[\frac{e\varphi_-(\rho,0)}{kT}\right]-1-\frac{e\varphi_-(\rho,0)}{kT}}. \tag{16}$$

We will not discuss possible solutions for Eq. (16) at small V for two reasons. First, we have already obtained this solution in Sec. III A and, secondly, as it will be shown later, the adiabatic approximation becomes inadequate in this limit. We restrict ourselves to the opposite limit of large $|V|$ when $e|\varphi_-(\rho,0)|\gg kT$. Contrary to the linear case, the solutions for V, $\varphi_-(\rho,0)>0$ (accumulation) and V, $\varphi_-(\rho,0)<0$ (depletion), differ dramatically. For the case of depletion, the right side of Eq. (16) is asymptotically proportional to $\sqrt{-\varphi_-(\rho,0)}$ and the equation has the solution

$$\varphi_-(\rho,0)=V-\frac{kT}{e}f(\rho)+\frac{kT}{e}\sqrt{f^2(\rho)-2f(\rho)eV/kT}, \tag{17}$$

$$f(\rho)=\frac{\varepsilon_2}{4}\ln^2\left(\frac{\sqrt{d+R}+\sqrt{d}}{\sqrt{d+R}-\sqrt{d}}\right)\lambda^2(\rho^2+d^2+Rd). \tag{18}$$

At large ρ this potential distribution is proportional to f^{-1} and hence decreases as ρ^{-2}. This is a steeper decrease than that for a linear potential (14), which ensures convergence and good localization of the resulting charge, and hence finiteness and good spatial resolution for the nonlinear capacity.

For large positive V analytical results can be obtained only in the limit $\varphi_-(0,0)/V\ll1$ and give

$$\varphi_-(\rho,0)=\frac{2kT}{e}\times\ln\left(\frac{\sqrt{2}eV}{\varepsilon kT\lambda\ln\left(\frac{\sqrt{d+R}+\sqrt{d}}{\sqrt{d+R}-\sqrt{d}}\right)\sqrt{\rho^2+d^2+Rd}}\right). \tag{19}$$

It is worth noting that the conditions $\varphi_-(0,0)/V\ll1$ and $e\varphi_-(\rho,0)\gg kT$ do not contradict each other. As it was shown in Sec. III A, the first of them is related to the system geometry and high dielectric susceptibility of semiconductor and does not imply smallness of V.

Equation (17) is the basic formula that we use in further calculations and for this reason it is important to check the applicability of the adiabatic approximation used in its derivation. To do this, we calculate the radial part of the Laplacian $\rho^{-1}\partial\varphi_-/\partial\rho+\partial^2\varphi_-/\partial\rho^2$ with φ_- given by Eq. (17), and require it to be much less than the right side of Eq. (11), equal to $4\pi en_0/\varepsilon$ in the region of complete depletion. The formula will contain the current value of ρ, which we replace with the characteristic $\rho_0 \equiv eV[\varepsilon kT\lambda \ln(\sqrt{d+R}+\sqrt{d}/\sqrt{d+R}-\sqrt{d})]^{-1}$ representing the radius of the complete depletion area, as determined from the expression $e|\varphi_-(\rho_0,0)|=kT$. The resulting condition for the validity of the adiabatic approximation is $e|V| \gg 2\sqrt{2}\ln(\sqrt{d+R}+\sqrt{d}/\sqrt{d+R}-\sqrt{d})\varepsilon kT$. For V measured by several volts this condition is usually fulfilled even at room temperature. For low-temperature measurements, a lower applied voltage can be used.

IV. CAPACITY CALCULATIONS

Once the potential distribution at the interface $\varphi_-(\rho,0)=\varphi_+(\rho,0)$ is determined, the tip capacity C can be found. Since, according to Eq. (12), $\varphi_-(\rho,0)$ is linearly related to $(\partial\varphi_-/\partial z)_{z=0}$, that is to the surface charge density in semiconductor, we have

$$C=\frac{1}{\ln\left(\frac{\sqrt{d+R}+\sqrt{d}}{\sqrt{d+R}-\sqrt{d}}\right)}\frac{d}{dV}\int_0^\infty \frac{[V-\varphi_-(\rho,0)]}{\sqrt{\rho^2+d^2+Rd}}\rho d\rho.$$

As has already been mentioned, the expression for C diverges (due to the first term in the integrand) and information on the doping level of a sample must be obtain from the differential characteristic

$$\frac{dC}{dV}=\frac{-1}{\ln\left(\frac{\sqrt{d+R}+\sqrt{d}}{\sqrt{d+R}-\sqrt{d}}\right)}\frac{d^2}{dV^2}\int_0^\infty \frac{\varphi_-(\rho,0)}{\sqrt{\rho^2+d^2+Rd}}\rho d\rho. \tag{20}$$

Let us apply this formula for particular potential distributions as calculated in the previous section. For large negative $\varphi_-(\rho,0)$, corresponding to the case of strong depletion and given by Eq. (17), we have

$$\frac{dC}{dV}=\frac{1}{\pi e\varepsilon n_0 \ln^3\left(\frac{\sqrt{d+R}+\sqrt{d}}{\sqrt{d+R}-\sqrt{d}}\right)\sqrt{d^2+Rd-\frac{V}{8\pi\varepsilon e n_0}\left[\ln\left(\frac{\sqrt{d+R}+\sqrt{d}}{\sqrt{d+R}-\sqrt{d}}\right)\right]^{-2}}}. \tag{21}$$

Equation (21) was derived with using the asymptotic formula (17), which is only applicable at sufficiently high values of $|\varphi_-(\rho,0)|$. For this reason we need to prove that the main contribution to the integral in Eq. (20) is given by the region of small $\rho<\rho_0$, where $e|\varphi_-(\rho,0)|>kT$. To do this, we note that the contribution from the undesirable region $\rho>\rho_0$ is given by a formula similar to Eq. (21), with d^2+Rd replaced by ρ^2. Thus, for our approach to be valid, we must require $[\varepsilon\lambda\ln[(\sqrt{d+R}+\sqrt{d})/(\sqrt{d+R}-\sqrt{d})]\rho]^2 \gg e|V|/(2kT)$. This is equivalent to $4e|V| \gg kT$ and is definitely fulfilled in our limit of strong depletion $e|\varphi_-(\rho,0)| \gg kT$.

The formula (21) is the central result of our theory and requires a special discussion. We note first that its dependences on both the applied voltage V and the doping level n_0, having at large bias the form $dC/dV \sim n_0^{-1/2}|V|^{-1/2}$, differ qualitatively from those of a planar Schottky diode, where $dC/dV \sim n_0^{1/2}|V|^{-3/2}$. This difference is due to two facts: the essentially non-one-dimensional potential distribution and a division of the applied voltage between the air backlash and the space charge region in the sample.

To demonstrate the role of these two contributing factors, we compare our formula with that for a reverse biased ($V<0$) planar metal-dielectric-semiconductor structure where the role of the dielectric is played by an air layer of thickness d_0. If the thickness of the depletion layer in the semiconductor is l, then the voltage drop in the semiconductor is $2\pi en_0 l^2/\varepsilon$, the electric field at the interface is $4\pi en_0 l/\varepsilon$, and the electric field in air is ε times larger. By assuming the total voltage drop is V, we obtain the quadratic equation for l: $l^2+2\varepsilon ld=\varepsilon|V|/(2\pi en_0)$. Since the charge density is $\sigma=en_0 l$, we obtain

$$\frac{dC}{dV}=S\frac{d^2\sigma}{dV^2}=\frac{S}{16\pi^2 e\varepsilon n_0\left(\sqrt{d_0^2-\frac{V}{2\pi e\varepsilon n_0}}\right)^3}, \tag{22}$$

where S is the device area.

If we ignore numerical constants and logarithmic factors, Eqs. (21) and (22) have some common features. They both are inversely proportional to n_0 and to some degree of the effective screening length d_{eff}, equal to the square root of the expression containing the dielectric thickness and width of depletion depletion layer, increasing with $|V|$. The essential distinction between SCM and a MOS structure is related to the fact that in the latter case the potential distribution is one dimensional and the device capacity is proportional to its area S. In the case of SCM, the region of charge variation is

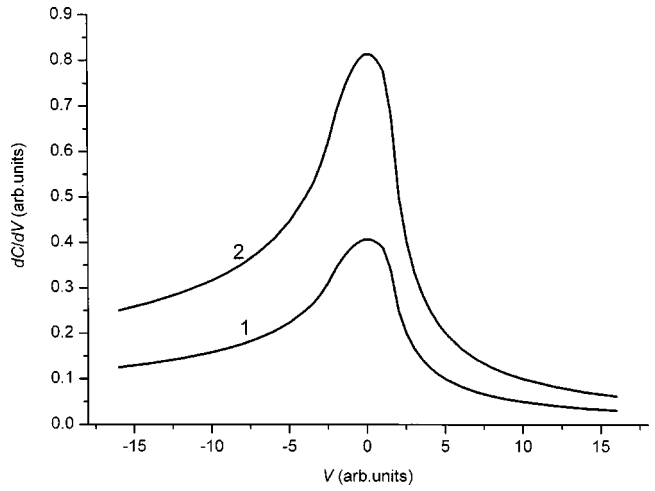

FIG. 3. Schematic voltage dependence of dC/dV for samples with two doping levels n_1 (curve 1) and n_2 (curve 2) where $n_1 > n_2$.

restricted in all dimensions by the effective screening length d_{eff} so that the role of S is played by d_{eff}^2. This changes the voltage dependence and results in a qualitatively different dependence of dC/dV on the doping level: at large depleting bias it decreases with n_0 in SCM geometry and increases for MOS structures.

Typically, SCM measurements are performed in the depletion regime but we present here calculations for accumulation voltage as well, since measurements in this regime were also reported in literature.[9] To derive dC/dV for the case of an accumulation potential, we must take Eq. (19), substitute it into Eq. (20) and integrate but not to $\rho=\infty$ (which, in any case, would diverge), but only to ρ_0 corresponding to $e\varphi_-(\rho,0)\simeq kT$. The expression for ρ_0 appears to be the same as that found above for the case of depletion, and

$$\frac{dC}{dV}\simeq\frac{\sqrt{kT}}{2e\sqrt{\pi n_0\varepsilon}V\ln^2\left(\dfrac{\sqrt{d+R}+\sqrt{d}}{\sqrt{d+R}-\sqrt{d}}\right)}. \tag{23}$$

Now we are in a position to understand behavior of dC/dV for all possible applied voltages. It is an asymmetric curve with a maximum, shown schematically in Fig. 3, which also agrees with the results of numerical simulation.[5] According to Eq. (21), at large depleting voltage it decreases $\sim|V|^{-1/2}$ and at large accumulation voltages decreases considerably faster, $\sim V^{-1}$ [Eq. (23)]. The maximal value of dC/dV is reached for a near zero bias. Though our formulas (21), (23) have an asymptotic character and are correct only at large bias, they allow us to establish a qualitative estimate for $dC/dV(0)$. The latter depends on the parameter $\lambda\sqrt{d^2+Rd}$. If $\lambda\sqrt{d^2+Rd}\gg 1$, then Eq. (14) gives

$$\varphi_-^{(1)}(0,0)=\frac{2V}{\varepsilon\ln\left(\dfrac{\sqrt{d+R}+\sqrt{d}}{\sqrt{d+R}-\sqrt{d}}\right)\lambda\sqrt{d^2+Rd}}.$$

This potential becomes comparable with kT/e at the critical voltage

$$V_c\sim(\varepsilon kT/e)\ln\left(\frac{\sqrt{d+R}+\sqrt{d}}{\sqrt{d+R}-\sqrt{d}}\right)\lambda\sqrt{d^2+Rd},$$

which determines the region of applicability (21) and (23). At $V\sim -V_c$ the last term in the argument of the square root in Eq. (21) is negligible, and the expression becomes voltage independent. Since the same expression can be also obtained for a positive bias by direct substitution of V_c, we can use it as an estimate for $dC/dV(0)$:

$$\frac{dC}{dV}(0)\simeq\frac{1}{\pi e\varepsilon n_0\ln^3\left(\dfrac{\sqrt{d+R}+\sqrt{d}}{\sqrt{d+R}-\sqrt{d}}\right)\sqrt{d^2+Rd}}. \tag{24}$$

For $\lambda\sqrt{d^2+Rd}\ll 1$, $\varphi_-^{(1)}(0,0)=V$ so that the role of V_c is played by kT/e. As a result, in Eq. (21) in the whole area of its applicability the term d^2+Rd can be neglected. As in the previous case, dC/dV at $V\sim\pm V_c$ has the same value for depletion and accumulation

$$\frac{dC}{dV}(0)\simeq\frac{1}{\sqrt{\pi\varepsilon n_0 kT}\ln^2\left(\dfrac{\sqrt{d+R}+\sqrt{d}}{\sqrt{d+R}-\sqrt{d}}\right)}. \tag{25}$$

V. SPATIAL RESOLUTION

One of the most important characteristics of any scanning probe technique is its spatial resolution. Though SCM may use the same equipment as STM or AFM, their resolutions differ by orders of magnitude. The probability of tunneling exponentially depends on the local distance between a tip and a sample and for properly prepared tips may drop dramatically at angstrom distances providing atomic scale spatial resolution. In SCM, resolution is determined by the spatial distribution of the electric field governed by the Laplace equation and its variation with coordinates is much slower. For this reason, the problem of SCM spatial resolution requires a special analysis.

As was mentioned above, SCM gives information on the electrical properties of a sample only when screening no longer has a linear character. The spatial resolution of SCM will be determined by the condiyion of when the size of region where the potential drop inside a semiconductor is large enough for nonlinear screening. If we successfully solve the problem formulated in Secs. II, III and find the potential distribution in the system, the spatial resolution in the radial direction $\delta\rho$ can be found from the equation

$$e|\varphi_-(\delta\rho,0)|=kT. \tag{26}$$

For large applied voltages, $\delta\rho$ coincides with the critical radius ρ_0 given above, so that

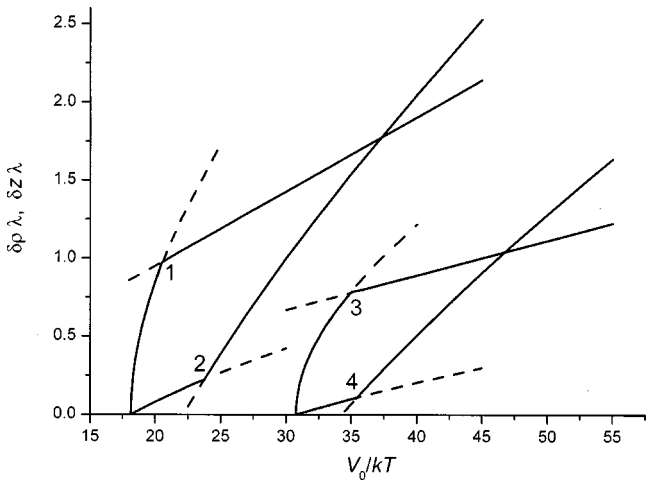

FIG. 4. Radial (1,3) and depth (2,4) resolution of SCM for the cases $d\lambda = R\lambda = 1$ (1,2) and $d\lambda = 1$, $R\lambda = 0.1$. The dashed lines represent the low- and high-voltage asymptotic behavior beyond the areas of their applicability.

$$\delta\rho \equiv e|V|\left[\varepsilon kT\lambda \ln\left(\frac{\sqrt{d+R}+\sqrt{d}}{\sqrt{d+R}-\sqrt{d}}\right)\right]^{-1}. \tag{27}$$

For small voltages, $\delta\rho$ is to be found numerically from the linear expression of Eq. (14). Figure 4 shows both answers for two different tip geometries. The solid lines are combined from these expressions, taken in their respective areas of validity, and demonstrate the real behavior of $\delta\rho$. It is natural that the in-plane spatial resolution should degrade ($\delta\rho$ increases) with the growth in applied voltage, since it is directly related to the expansion of the space charge region.

By comparison, it would be interesting to calculate the depth resolution of the method δz as determined from the condition $e|\varphi_-(0,-\delta z)| = kT$. To find δz for large applied voltages, we note that Eq. (15) is the first integral of the Poisson equation (11) in the adiabatic approximation, and is valid not only at $z=0$ but also at any $z<0$. Assuming $\rho = 0$ and integrating over z again, we have for the case of a depleting potential ($V<0$):

$$\delta z = \frac{1}{\sqrt{2}\lambda}\int_{e\varphi_-(0,0)/kT}^{-1} \frac{dt}{\sqrt{\exp(t)-t-1}} \tag{28}$$

with $\varphi_-(0,0)<0$ given by Eq. (17). For small voltages, δz is found from Eq. (14), as well as $\delta\rho$. These results are also presented in Fig. 4. One can see that for small bias, the in-plane resolution of SCM is considerably worse than the depth resolution, but for large depletion bias, resolution in both directions become comparable and, moreover, the in-plane resolution becomes even better than the depth resolution.

VI. CONCLUSIONS

In this paper we developed a theory for SCM, a powerful method for measuring the spatial distribution of doping levels in semiconductors. The analysis shows that, contrary to the standard capacity measurements made using bulk Schottky contacts, the capacity itself is determined by the macroscopic geometry of the sample and by the measuring instrument, and hence can not be used for a local determination of the doping concentration. The latter can be found only by using a modulation technique for measuring the derivative dC/dV.

It is worth noting that, besides measurements of dC/dV, there exists another modulation technique, namely, scanning capacitance force microscopy (SCFM),[10] based on the modulation of the distance d and measuring the force, proportional to $dC/d(d)$. It can be seen from Eq. (7) that this derivative, as well as C itself, is determined by large ρ and diverges for an infinite sample. This explains why the modulation of only d does not allow us to measure local sample characteristics, and voltage modulation is necessary in SCFM as well.

Analytical calculations show that dC/dV depends on the applied voltage V nonmonotonically, having a maximum at zero bias. At large positive (accumulation) bias it decreases $\sim V^{-1}$ while for large negative (depletion) bias the decrease is less steep, proportional to $|V|^{-1/2}$. The slope of the linear $(dC/dV)^{-2}$ versus V dependence is proportional to the doping concentration n_0 and can be used for its determination.

The spatial resolution of SCM is incomparable with the resolution of STM and AFM with the same tip geometry, and is determined by the screening length within a semiconducting sample. The resolution increases with applied bias due to the growth of the region of nonlinear screening.

ACKNOWLEDGMENT

The authors gratefully acknowledge D. Pelinovsky (McMaster University) for useful discussions.

*Email address: shik@ecf.utoronto.ca

[1] C. C. Williams, Annu. Rev. Mater. Sci. **29**, 471 (1999).
[2] Y. Huang and C. C. Williams, J. Vac. Sci. Technol. B **12**, 369 (1994).
[3] J. S. McMurray, J. Kim, and C. C. Williams, J. Vac. Sci. Technol. B **15**, 1011 (1997).
[4] J. J. Kopanski, J. F. Marchiando, and J. R. Lowney, Mater. Sci. Eng., B **44**, 46 (1997).
[5] J. F. Marchiando, J. J. Kopanski, and J. R. Lowney, J. Vac. Sci. Technol. B **16**, 463 (1998).
[6] D. B. Balagurov, A. V. Klyuchnik, and Y. E. Lozovik, Phys. Solid State **42**, 371 (2000).
[7] C. Flammer, *Spheroidal Wave Functions* (Stanford University Press, Stanford, CA, 1957).
[8] M. Abramowitz and I. A. Stegun, *Handbook of Mathematical Functions* (NBS, Washington, 1972).
[9] M. von Sprekelsen, J. Isenbart, and R. Wiesendanger (unpublished).
[10] K. Kobayashi, H. Yamada, and K. Matsushige, Appl. Phys. Lett. **81**, 2629 (2002).